Original Research Article

Parameters controlling the uranium mineralization in the Ingall sector, Tim Mersoï basin (Northern Niger)

Abstract

This study focuses on highlighting and controlling of uranium mineralization in the Ingall area (Northern Niger). The study sector is an integral part of the Tim Mersoï basin located to the northern part of the Iullemenden syneclise. Located on the western edge of the Aïr Massif, this basin, known for its uranium mineralizations, has a sedimentary filling ranging from Devonian to Lower Cretaceous. All the sedimentary formations of this basin end in a bevel on the western edge of the Aïr Massif. To carry out this study, the radiometric airborne geophysics technique was first deployed to highlight surface uranium anomalies. These were then verified by ground radiometry technique. The mapping work then identified the major geological structures that controlled the emplacement and distribution of the mineralization. Drilling and logging techniques were used to determine the mineralization host formations, the Assaouas and Tchirezrine-2. The results of this work show that the uranium mineralization in the Ingall sector occurs as lenticular ore bodies. Tectonic structures (normal faults), palaeogeography and chemical elements (reducing elements) are the main factors controlling the concentration and distribution of this mineralization. This study shows that this area, underestimated for decades, is potentially rich in uranium mineralization.

Keywords: Tim Mersoï basin, Ingall sector, Uranium mineralization, Tectonic control, Palaeogeographic control, Chemical control.

1. Introduction

The Ingall sector belongs to the Tim Mersoï uranium basin in northern Niger. This basin, located on a stable lithosphere, is a good example of an intracratonic basin with a low average subsidence rate and preserved over a long period (Gerbeaud 2006; Mamane 2016). For several years, the Tim Mersoï basin has been the subject of uranium exploration and exploitation campaigns (Wagani 2007). This is how many uranium deposits have been identified, others of which are already in operation (COMINAK, SOMAÏR, SOMIDA). In the Ingall sector, signs of uranium mineralisation were discovered during the airbone geophysical campaign (TRPAD Azelick) between 1959 and 1960 which revealed surface mineralisation (Sanda et al. 2022). However, this sector has been neglected in favour of other sectors deemed more profitable. Nevertheless, as geologically continuous with other uranium sectors (IMOURAREN, AZELICK) in the Tim Mersoï basin, this sector has recently been the subject of a mining exploration campaign. The Ingall sector is now considered promising through its location at the west of the Arlit flexure-fault, like many discovered uranium deposits in the Tim Mersoï basin (COMINAK, SOMAÏR, IMOURAREN, Moradi) (Forbes 1989; Gerbeaud 2006; Mamane 2016; Sanda et al. 2022). The mineralization being observed on the surface, it was therefore necessary to determine the dip of the anomaly at depth and the host formations.

The objective of this study is to determine the factors that controlled the emplacement and distribution of uranium mineralization in the Ingall area. Thus, airborne and ground radiometric surveys are used to identify areas of surface anomalies. Then, the spatial distribution of the mineralization and its controlled geological structures, were apprehended through the geological mapping work. Finally, the drilling and logging data made it possible to understand the vertical extension, the plunge, the emplacement pattern and the host formations of the uranium mineralization in the Ingall sector.

2. Geological setting

The Ingall sector (Northern Niger) (Figure 1) is an integral part of the Tim Mersoï basin which is belonging to the Iullemenden syneclise. The Tim Mersoï basin is limited to the east by the Aïr Massif, to the north by the Hoggar, to the west by the In Guezzam ridge and to the south by the Iullemenden basin in the strict sense (SS) (Valsardieu 1971). The Pan-African age Aïr Massif was formed by an intensely deformed set of metamorphosed rocks migmatic crossed by numerous syn-tectonic, late-tectonic and post-tectonic ancient granites (Konaté et al. 2019). The sedimentation history of the western edge of the Aïr (Tim Mersoï basin) is mainly marked by marine transgressions (Joulia 1963). This basin is made up of Palaeozoic and Intercalary Continental deposits of the Permian to Lower Cretaceous age (Valsardieu 1971). In this region, significant sedimentation would have started in the Paleozoic where the sedimentation areas would have been confined to the Tin Seririne syncline from the Cambro-Ordovician (Moussa 1992). There was a shift of deposits from the northeastern to the southwestern, related to the migration of the subsidence pole of the Iullemenden Basin during the Early Paleozoic-Cretaceous period (Greigert and Pougnet 1967). The sediments thickness in the Tim Mersoï basin is up to 1300 m deep (Moussa 1992; Sani et al. 2020). Along the western edge of the Aïr, the sedimentary formations are successively bevelled and the oldest one rests directly on the crystalline and crystallophyllous basement of the Aïr (Moussa 1992). On the eastern edge of the Tim Mersoï basin, movements of the inherited basement structures affect the sedimentary cover (Konaté et al. 2007). General shearing deforms the basement along very specific directions and propagates into the cover. The sedimentary layers dips are very slightly to the west and the numerous deformations that affect them are the attenuated reflection of the dislocations of the underlying basement and are expressed in the form of flexures and flexure-faults (Gerbeaud 2006). Among these structures, the Arlit-In Azaoua normal flexure-fault (N-S) has regional importance. It separates the Tim Mersoï basin into two major compartments (East-Flexure and West-Flexure compartments). Throughout its North-south extension, the geometry of this regional fault and its vertical rejection vary in proportions. On a large scale, rejection reversals are also observed (Gerbeaud 2006).

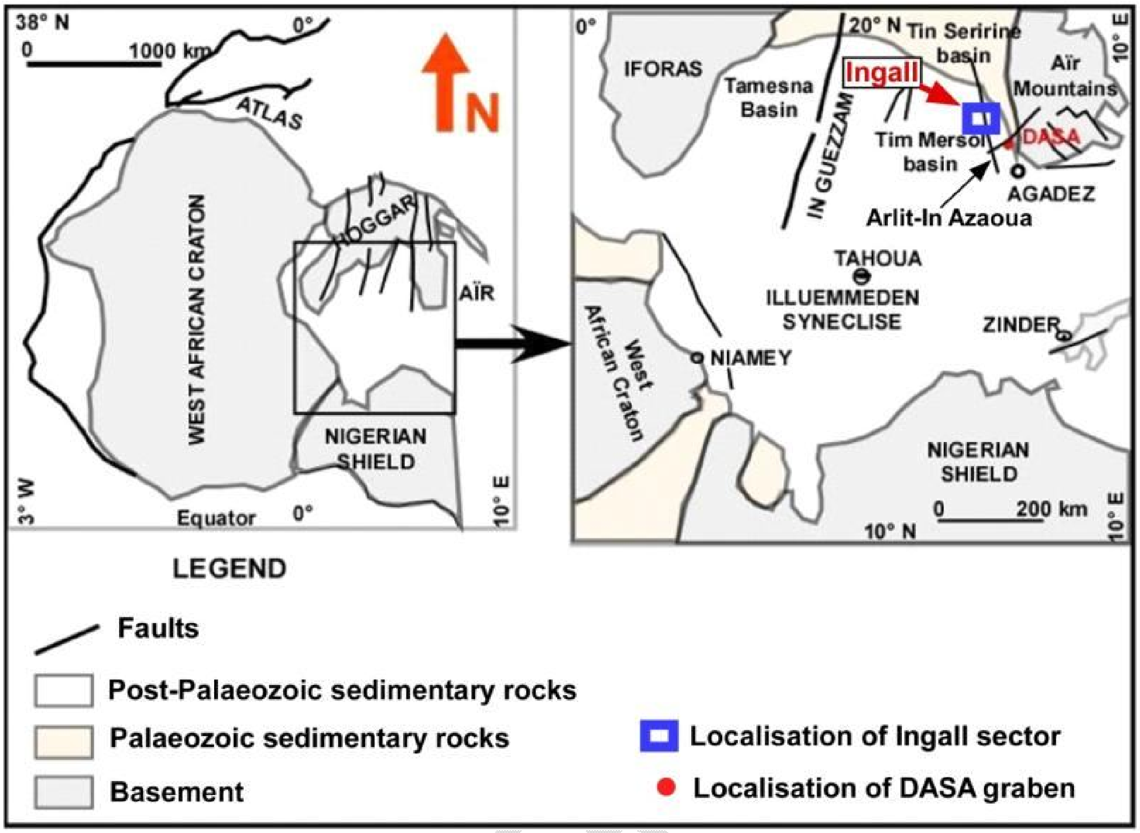

Fig 1. Geographical location of the Tim Mersoï basin and Ingall sector in the Iullemmeden syneclise (Modified from Sani 2020).

At the edge of the Aïr, the Cambro-Ordovician to Cretaceous age sedimentary cover comprises a periodic succession of sedimentary environments with marine and continental trends (Figure 2). The following stages and series have been observed:

- The Precambrian: during this period, the western edge of the Aïr consists of ancient calc-alkaline granites with some intrusive batholiths, alkaline to hyper-alkaline granites;
- The Carboniferous: it is subdivided into 3 series: the Teradah, Lower Tagora (Lower Carboniferous) and Upper Tagora (Upper Carboniferous) series. Each of these series begins with a sandstone formation, fluvio-glacial at the Teragh formations, fluvio-deltaic at the Guezouman in the Lower Tagora (with the radioactive conglomerate of Teleflak at its base) and Tarat in the Upper Tagora;
- The Permian: essentially continental, consisting of two powerful red sandstone bars (Izegouande and Téloua-2 and 3) interleaved with several levels of red-brown siltstones (Téjia, Tamamait, Moradi);
- The Triassic: represented by the fine-grained sandstones of Téloua-1, covers the Anou-Melle conglomerate;
- The Jurassic: this includes the fluvial sandstone formations of Téloua-2 and 3, Tchirezrine-1 and 2, with lacustrine interlayers (Mousseden). These formations, which locally contain analcime levels, are only known to the south and west of the Arlit sector;

- The Cretaceous: constituted by the clayey lacustrine formation of the Irhazer, at its base with the silty and fine-grained sandstone levels of the Assaouas.

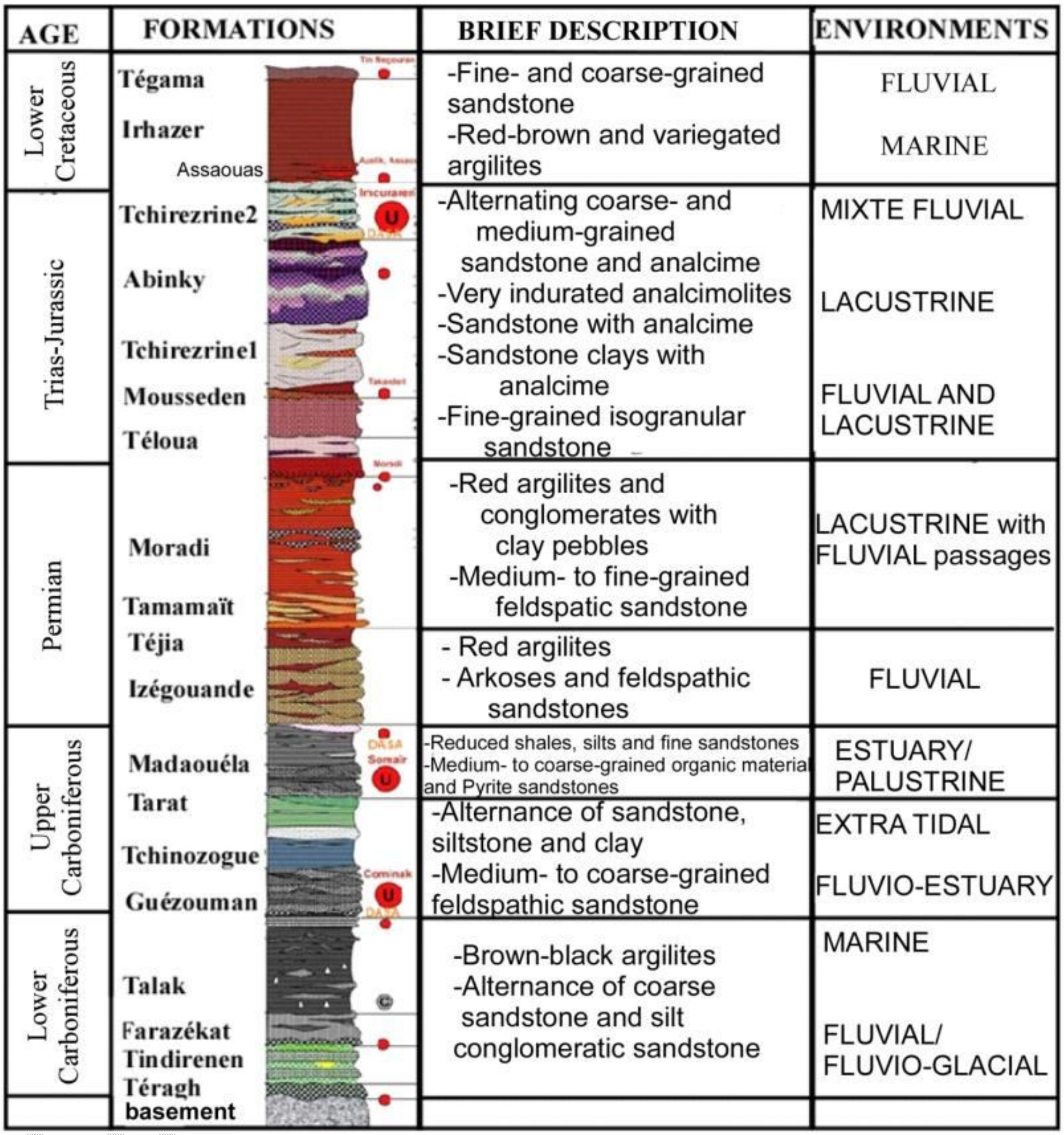

Fig 2. Regional lithostratigraphic column of the Tim Mersoï basin (Sani 2020).

3. Material and methods

To achieve the objectives of this work, a multidisciplinary approach including airborne geophysics, ground radiometry, geological mapping, destructive drilling, lithological description and loggings was implemented.

(i) Radiometric airborne geophysics or gamma-spectrometry was carried out initially to delineate the anomalous areas of the study area. A gamma-spectrometric sensor was flown in an helicopter over the study area with a flight height of approximately 150 m and an average speed of 80 km/h. This geophysical investigation identified areas of considerable anomaly (over 100 cps) at the surface and subsurface.

(ii) The anomaly areas identified by the airborne geophysics were verified on the ground by the ground radiometric method using a spectrometer (Figure 3A). This device captures the gamma radiation flux and gives the value in shocks per second (cps).

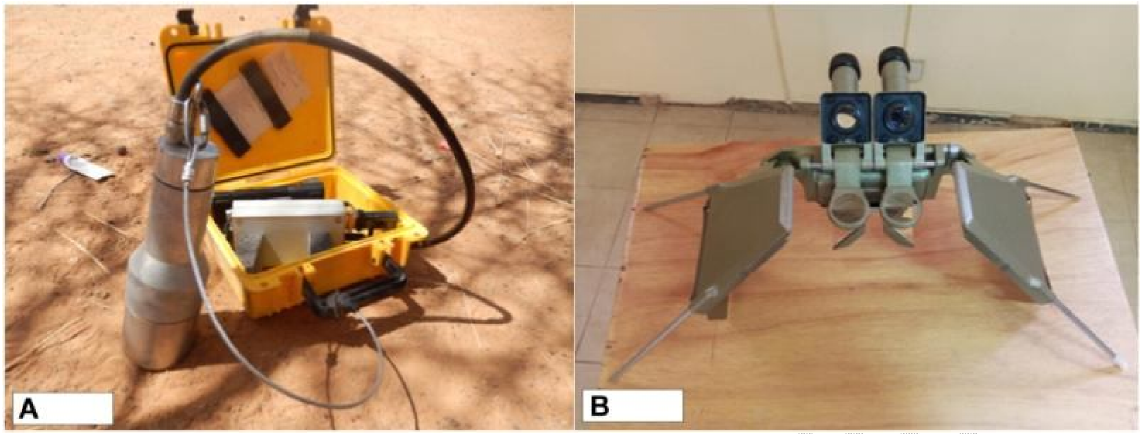

Fig 3. (A) Gamma spectrometer. (B) Geoscope-type stereoscope.

(iii) The anomalous tested areas were geologically mapped. The various outcropping lithofacies were described and the major local geological structures were identified. The geological map is completed with lineaments extracted through aerial photographs using a stereoscope (Figure 3B) and mapping softwares (Arcgis 10.8 and Canvas 11).

(iv) Destructive reconnaissance drilling was then carried out in the anomalous zones to verify the vertical extension of the anomaly. In areas where surface mineralization has not been identified, the drilling is used to verify its existence at depth and identify the host formations.

(v) The cuttings were collected and described. The description of the cuttings made it possible to determine the lithological characteristics of the formations crossed by the various drillings.

(vi) Logging measurements were made directly after each borehole was drilled. The Geovista equipment was used for these operations (Figure 4A). At the end of these operations, crucial and accurate informations about the surveys are obtained. These are:

- Tilt and azimuth with the VERT probe. This probe is 0.52 m long, 38 mm in diameter and weighs 2.5 kg. It measures the vertical inclination of the borehole concerning magnetic north and the azimuth over 360° with an accuracy of 0.4° and 2° respectively.
- The hole diameter with the CAL3 probe (Figure 4B). Also known as the Calliper, this three- armed, 1.37 m long, 38 mm diameter, 8.5 kg probe measures the hole diameter with an accuracy of 5 mm and a resolution of 0.01 mm.
- Resistivity (with the DLL3 probe): this resistivity is 2.27 m long, 38 mm in diameter and weighing 7.5 kg. It probe uses high-capacity electrodes to measure near and deep resistivity with good resolution.
- Natural radioactivity or natural gamma by the NGRS probe. This probe has a scintillation device. The probe weighs a total of 4 kg for 0.7 m in length and 38 mm in diameter. It is accompanied by a Geiger-Muller device when the content exceeds 2000 cps.

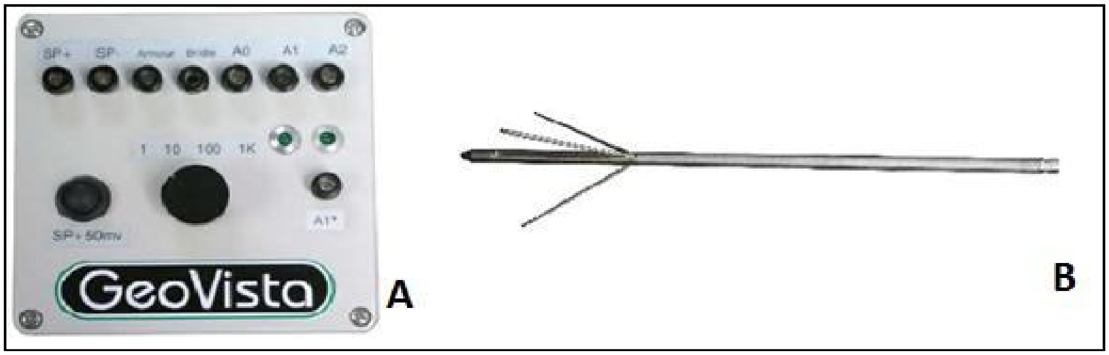

Fig 4. (A) Calibration and resistivity test box. (B) Three-arm calliper tool.

4. Results and discussion

4.1. Radiometric survey

The results of the airborne geophysics generated a radiometric map of the Ingall area (Figure 5). Analysis of this map shows variable uranium values (5 cps to over 200 cps). At the 100 cps to 200 cps cut-off, two envelopes of uranium anomalies can be distinguished in the centre of the study area (Figure 5). These anomalies, identified by airborne geophysics, were confirmed by the ground radiometric method (Figure 5) with observed discontinuous distribution of this surface mineralization.

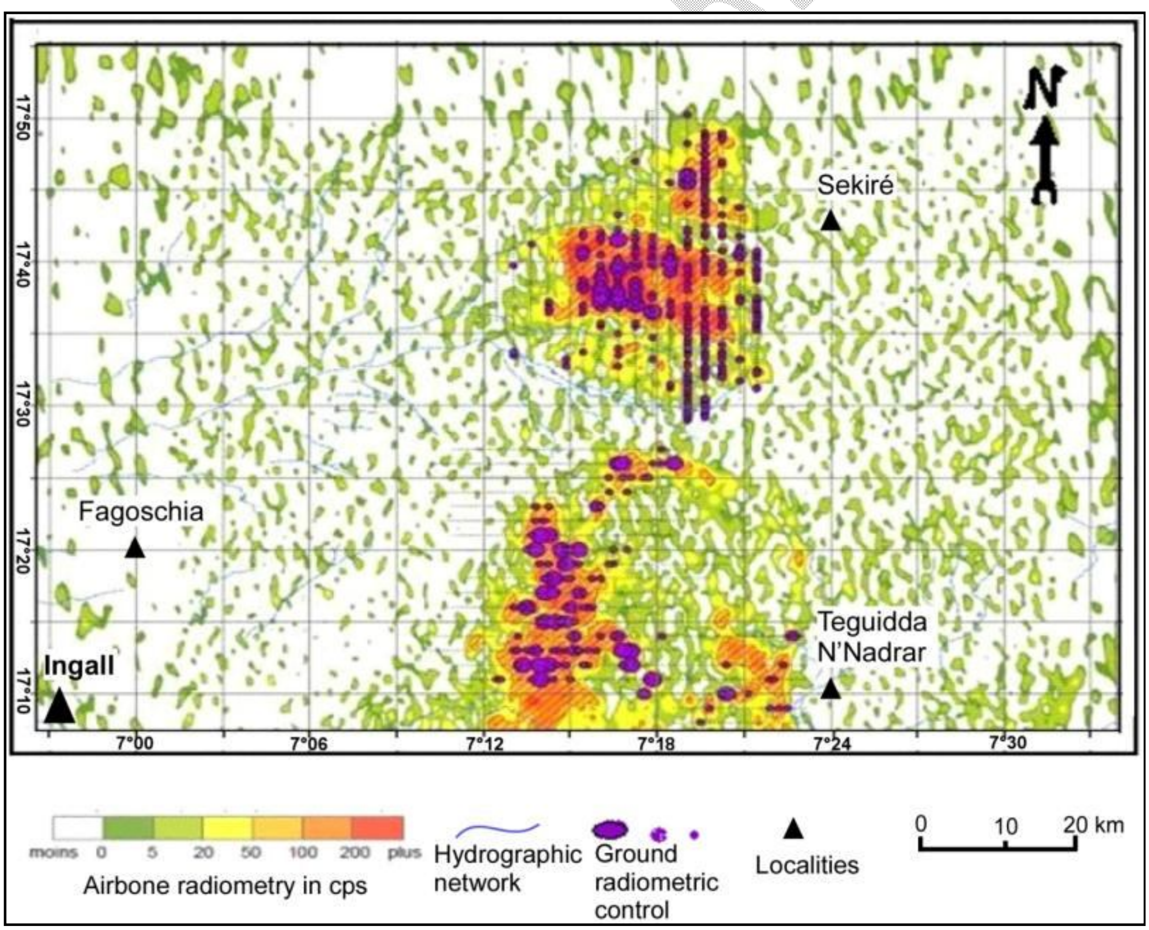

Fig 5. Radiometric map of the Ingall area.

4.2. Geological mapping

The geological mapping carried out in the Ingall sector consisted of a lithological description of the outcropping formations and a survey of the major geological structures. This activity revealed three sedimentary formations outcrop in the study area namely the Irhazer claystone, the Assaouas fine-grained and the medium-grained sandstone to coarse-grained sandstone of Thirezerine-2.

- The Irhazer claystone outcrops to the east and west of the Ingall area. These outcrops are characterized by reddish to greenish carbonate claystone. The Irhazer formation is slightly sandstone with an abundance of very fine-grained sandstone at the base. This formation is sometimes overlain by sandstone and conglomeratic alluvium.
- The Assaouas outcrops to the hinge part of the study area. These outcrops are made by fine-grained or analcimonious sandstones. The Assaouas outcrops are also characterized by a calcareous level which is often indurated with a slab-like flow.
- The Tchirezrine-2 outcrops above all to the south of the central part of the Ingall sector. It is a formation of medium-grained to coarse-grained sandstone with clay or analcimony cement.

Major geological structures of the study area, were carried out through regional geological map (Figure 1), aerial photos (Figure 6) and field observations (Figure 8). The Arlit-In Azaoua flexure-fault of regional extension is the main major structure that crosses the study area in a globally N-S direction (Figure 1). It is a syn-sedimentary normal fault (Forbes 1989; Gerbeaud 2006; Konaté et al. 2007; Sani 2020; Sani et al. 2022). The interpretation of aerial photographs made it possible to extract a network of lineaments from the study area. These lineaments help us to verify the passage of the Arlit-In Azaoua flexure-fault (N-S) and its rejects (N-S, N20°E, N70°E, N100°E) through the Ingall sector and to complete the geological map (Figure 7). The main Arlit-In Azaoua fault and the secondary fractures have been confirmed by field observations (Figure 8).

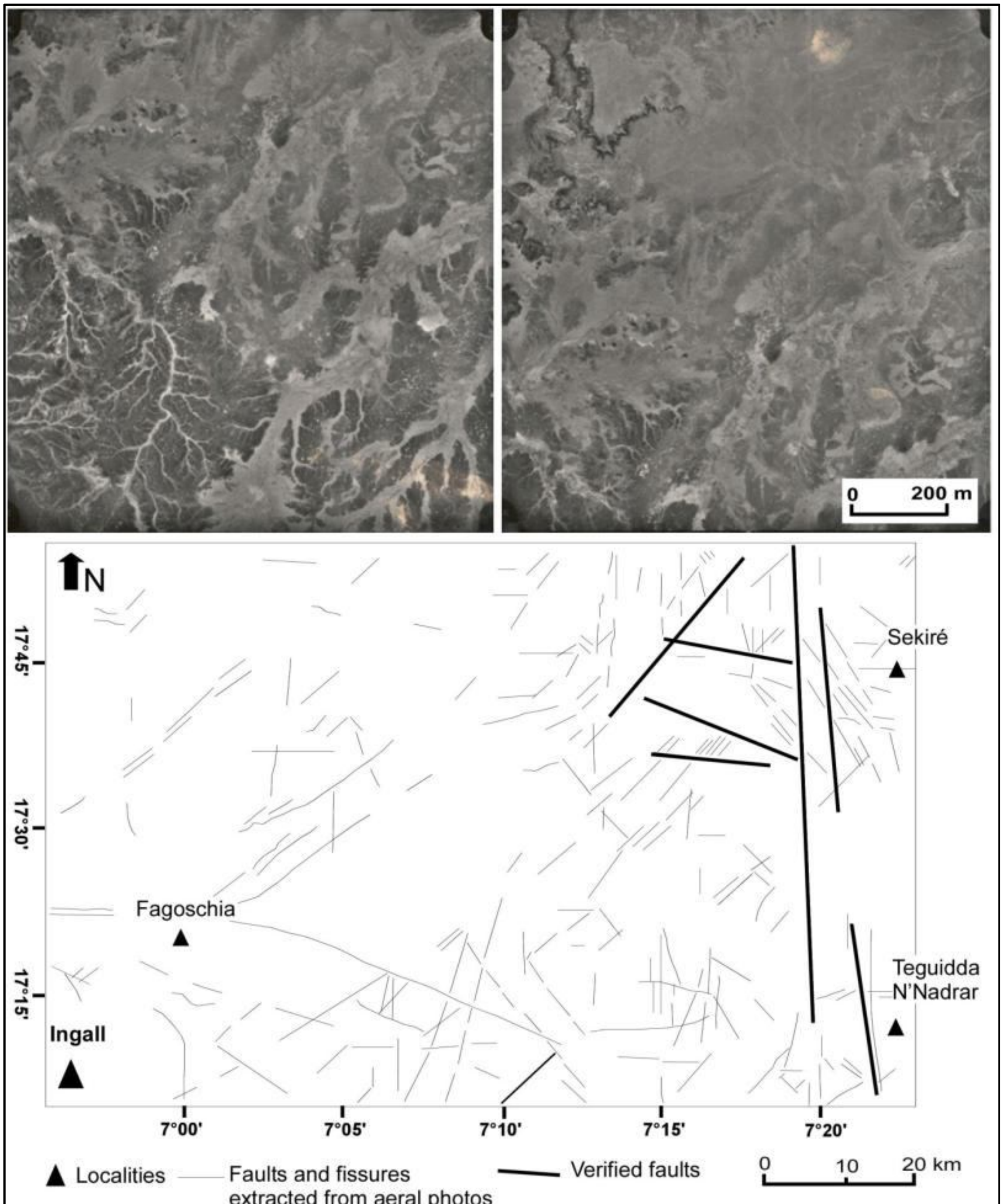

Fig 6. Example of aerial photos used to carry out lineaments map.

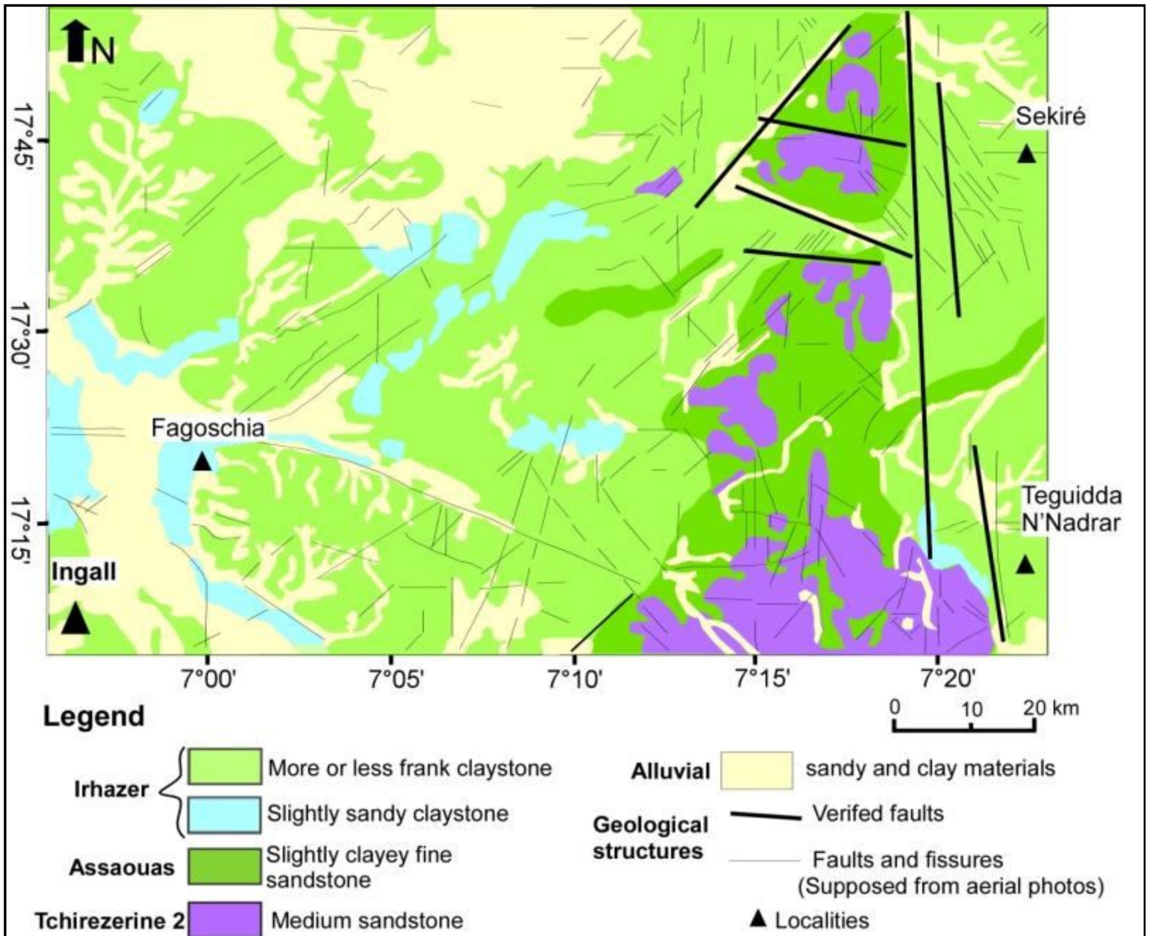

Fig 7. Geological map of the Ingall area.

The major geological structures in the study area are the Arlit-In Azaoua regional flexure-fault, secondary faults (N-S, N20°E, N70°E, N100°E) and a local dome (Figures 7 and 8). The large Arlit-In Azaoua structure crosses the Ingall sector along its entire N-S length and divides the sector into two parts: East and West. The rejection of the fault is manifested in the east by significant thicknesses of Irhazer formation. To the west of the Arlit-In Azaoua flexure-fault, there is a thickening of the Irhazer formation. However, this considerable thickness is rather due to a significant filling of the Tim Mersoï basin in this sector by this Irhazer formation. This thickening has led to the formation of an N-S anticline or dome (Figure 8B) parallel to the flexure-fault. A-A' and B-B' cross-sections (Figure 8C) in the anomalous area show horst structure inherited from secondary faults (Figure 8A). The high elevation of the graben zone exposes the Irhazer formation to severe erosion. This structural arrangement is comparable to the DASA N70°E graben where a syn-sedimentary clay filling of the central part of the graben is demonstrated. However, at the level of this DASA zone, the edges of the graben present only very small thicknesses. These structuring, observed at the level of Ingall and DASA, are inherited from the great basin of Tim Mersoï which shows a dome and gutter structures (Konaté et al. 2007).

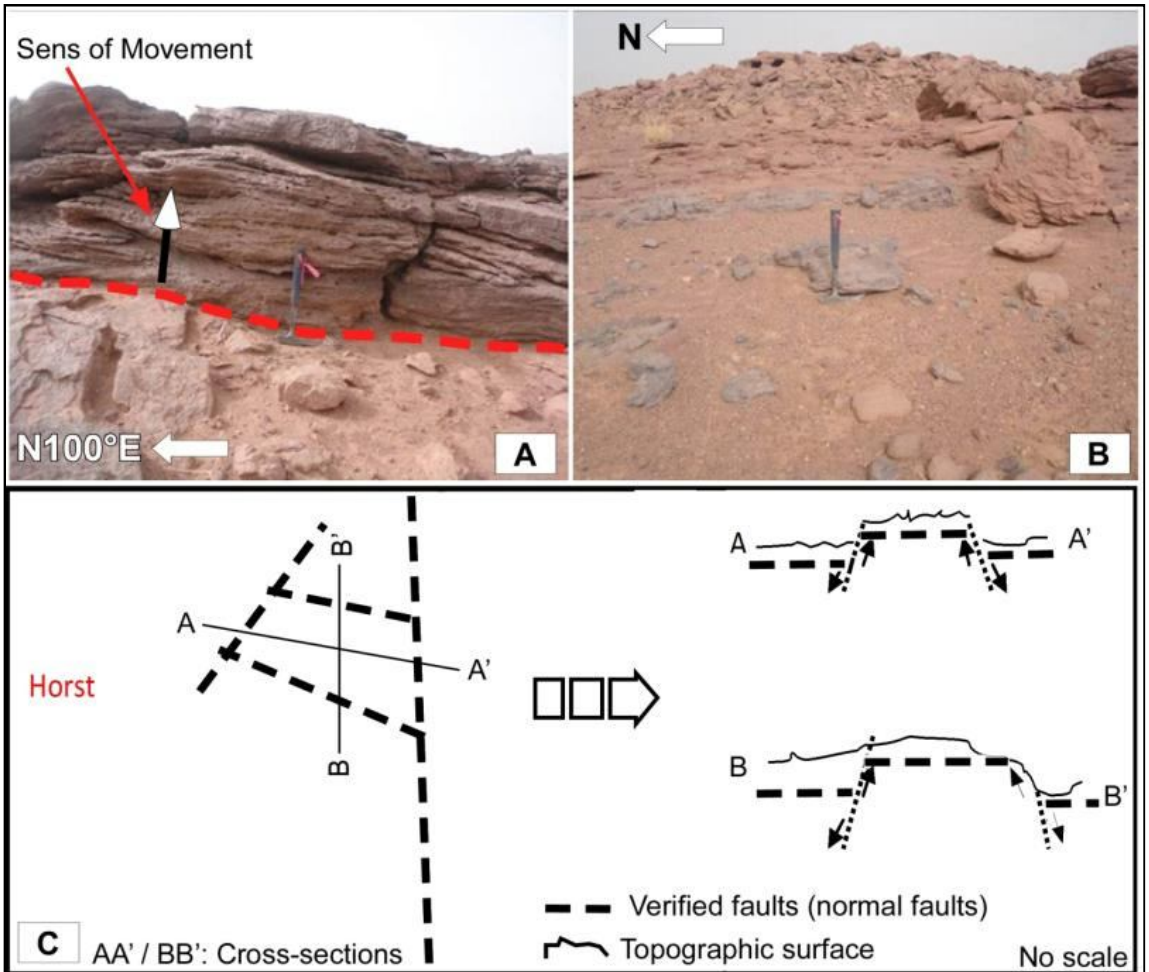

Fig 8. (A) Normal fault N100°E. (B) Dome N-S. (C) Sketch showing the formation of the horst by normal faults.

4.3.Interpretation of the spatial distribution of uranium mineralization

The horizontal distribution of the uranium mineralization shows that the anomalous zones are located in the central part of the study area in a generally N-S direction. The geological mapping shows that the outcropping formations in the anomalous zones are essentially made up of the Assaouas and Tchirezrine-2 formations (Figures 5 and 7). However, in the areas with low uranium anomalies, only hosted in the Irhazer formation outcrops (Figures 5 and 7). As this formation is stratigraphically above the Assaouas and Tchirezrine-2 formations, it would have masked the positively radiometric responses to the east and west of the anomaly. The Assaouas and Tchirezrine-2 formations would then be the host formations for the uranium mineralization in the Ingall area, as observed at IMOURAREN (Billion 2014) and DASA (Sani 2020). The anomaly area is further bounded to the east by the Arlit-In Azaoua regional flexure-fault, to the west by the N20°E secondary fault, to the north and the south by the N70°E to N100°E secondary faults. These structures have also subdivided the anomaly into two to three envelopes. The interpretation of these different structural arrangements clearly shows that this surface anomaly has been structurally controlled. This is the case for several uranium deposits discovered in the Tim Mersoï basin (SOMAÏR, COMINAK, IMOURAREN, DASA) (Forbes 1989; Gerbeaud 2006; Konaté et al. 2007; Sani et al. 2020;

Sani 2020). In the Ingall area, normal faults have compartmentalized the anomalous zone into horsts and grabens. The horsts constitute the envelope zones of surface anomalies. In these areas, the Irhazer formation has been raised and eroded, resulting in the outcrop of the Assaouas and/or Tchirezrine-2, which are host mineralization formations. Furthermore, it should be noted that this surface anomaly is very discontinuous across the study area. This high variability in uranium content is probably related to the effects of surface erosion, which is very dynamic in this area (Figure 9).

Fig 9. Outcrop of Assaouas formation showing significant alteration and product of erosion in the Sekiré sector (Figure 7).

4.4.Analysis and interpretation of drilling and logging results

To verify the existence of the uranium anomaly at depth, destructive drilling was carried out in the surface areas of anomalous and unmineralised zones. Two E-W cross-sections namely A-B and C-D, were drilled systematically (Figure 10). Data from drilling (lithological description) and logging (uranium grades) were used to characterize the horizontal and intra-formation distribution of the mineralization. Drilling was carried out in such a way that it crossed the Irhazer, Assaouas and Tchirezrine formations. All drilled holes were stopped a few metres at the Abinky formation which is not mineralised. This formation is made up of hardened analcimolites with intercalations of claystone and fine-grained sandstone. It should be noted that all the drilled holes are negative to the east of the flexure-fault.

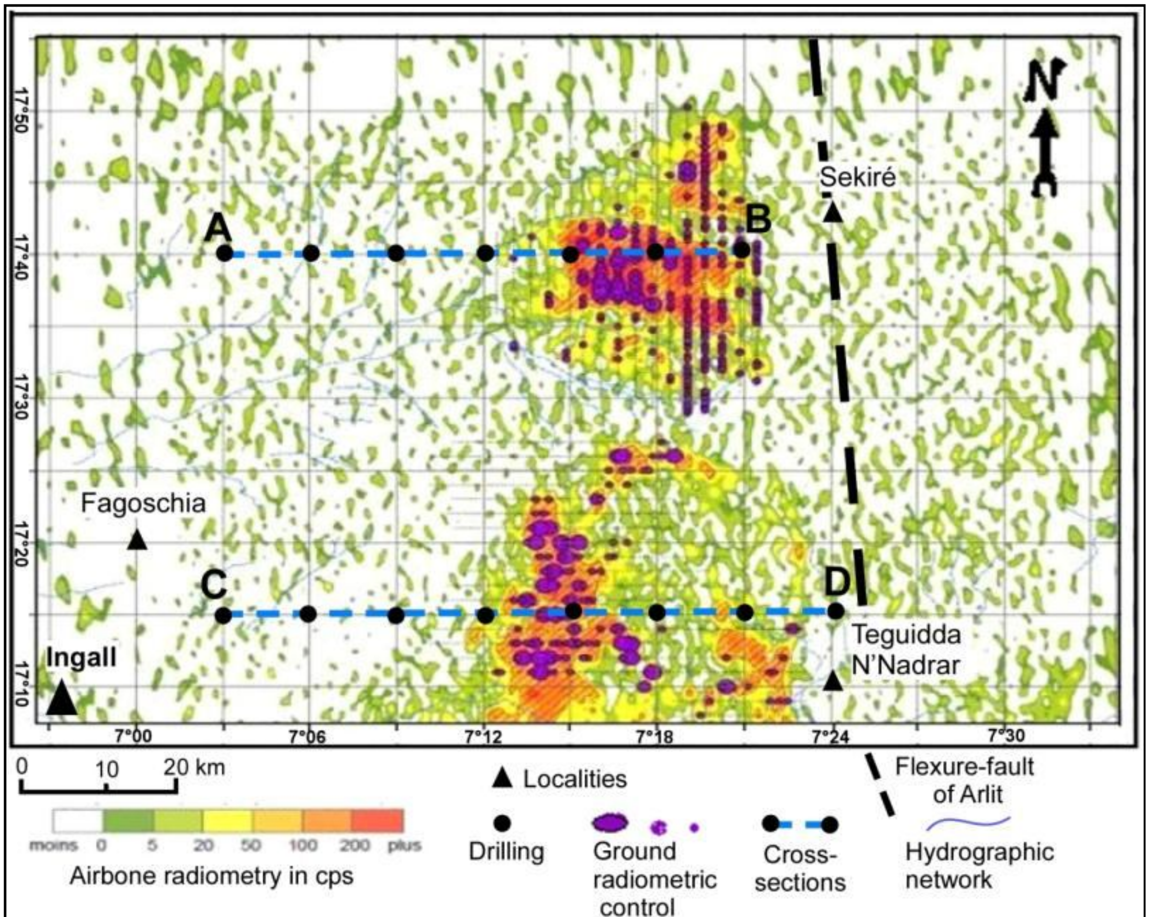

Fig 10. Location of cuttings and drilled holes in the study area.

4.4.1. A-B cross-section

The A-B cross-section was completed to the north of the study area (Figure 10). All drilled holes intersected by this cross-section are positive grades ranging from 5 to over 200 cps. In the drilled holes in the east of the A-B cross-section, the mineralization is situate at the top and then dips to the west (Figure 11). This mineralization distribution is in agreement with the radiometric surveys and geological mapping which have highlighted surface anomalies in the Assaouas and Tchirezrine-2 formations, on the western edge of the Arlit flexure-fault (Figures 5 and 7). All drilled holes show the mineralization is exclusively hosted in the entire thickness of the Assaouas formation and the upper part of the Tchirezrine-2 formation (in the medium-grained to coarse-grained sandstones and analcimolites) (Figure 11).

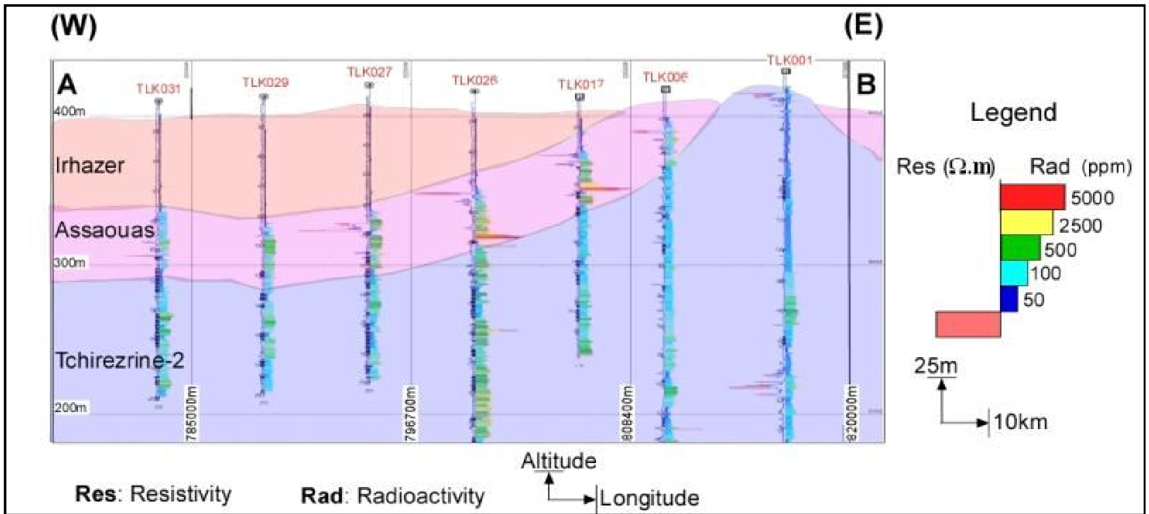

Fig 11. A-B cross-section.

4.4.2. C-D cross-section

Cross-section C-D (Figure 12) is located in the south of the study area (Figure 10). All the drilled holes show grades ranging from 5 to over 200 cps. In the central part of the cross-section, the mineralization is observed in the top of drilled holes, whereas to the east and west, the mineralization dips. This condition agrees with the results of the radiometric surveys and geological mapping which show the existence of surface mineralization in the Assaouas and Tchirezrine-2 formations. These two formations, outcrop in the central part of the study area due to structural control (grabens). At the top of C-D cross-section, all the drilled holes show positive grades of uranium mineralization which is hosted in the Assaouas and Tchirezrine-2 formations.

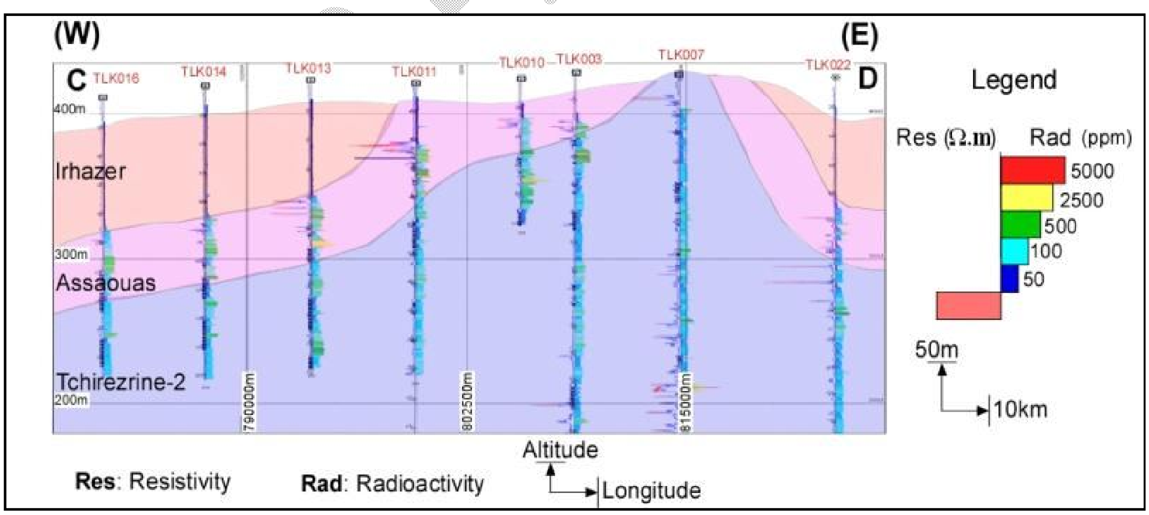

Fig 12. C-D cross-section.

4.5.Discussion on the mineralization found

The grades of uranium mineralization identified in the various boreholes by gamma logg were used to draw the envelopes of mineralization in depth with the cut-off of 500 ppm to 5000 ppm (0.05% to 0.5%). Figure 13 shows that both vertically and horizontally uranium mineralization is discontinuous in the Ingall area. The mineralization is lens-like ore bodies (Figure 13).

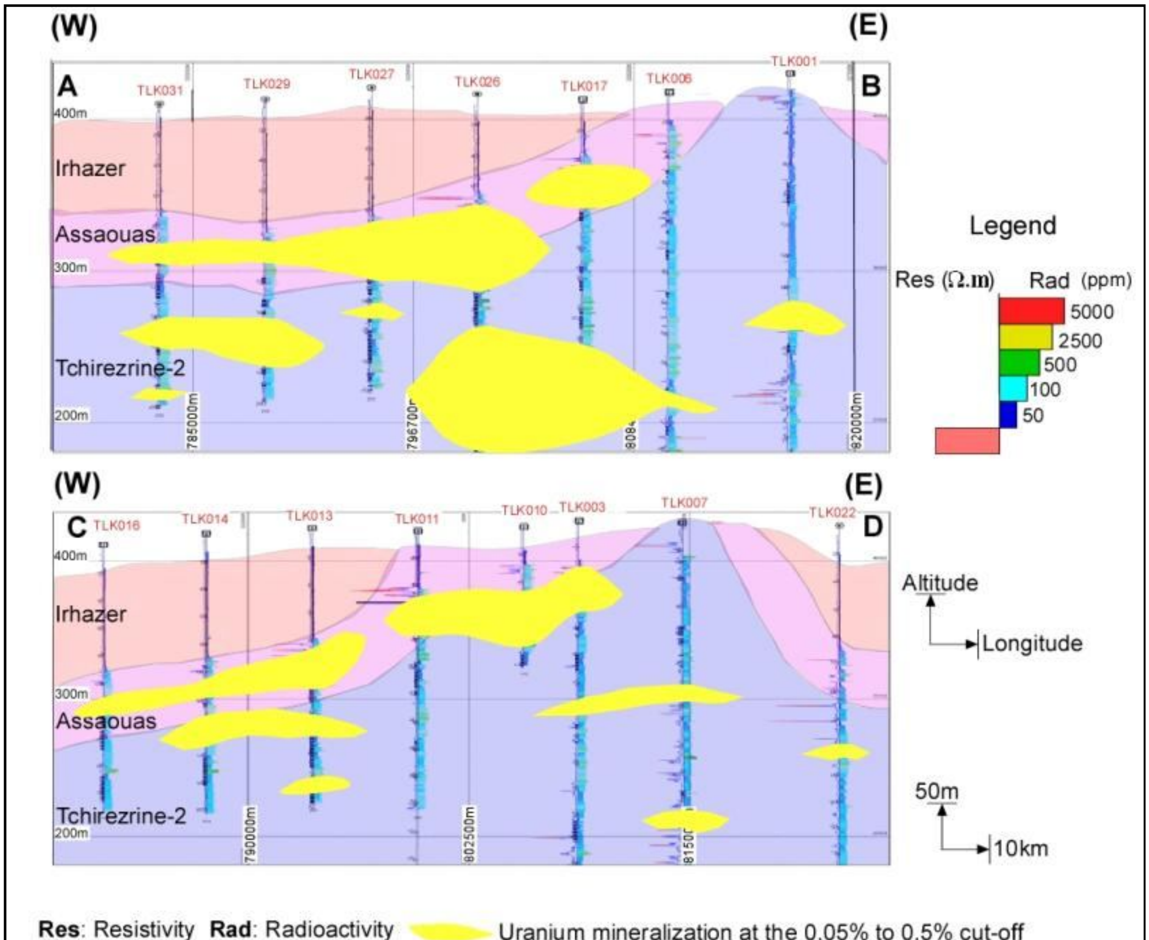

Fig 13. Uranium mineralization envelopes as lenses at the 0.05% to 0.5% cut-off.

This lenticular ore bodies of uranium mineralization found in the Ingall area is similar to several mineralizations in the Tim Mersoï basin (Gerbeaud 2006; Sani 2020). Such deposits would be formed through erosion of primary mineralized zones by channels which transport uranium in solution, in the oxidized state. Thus, the mineralized fuilds fills irregular gorges or depressions in the downstream zone (Moussa 1992). These gutters are the preferential places for the deposition of chemical elements and minerals with a reductive vocation (pitchblende, coffinite) which can thus fix uranium (Salze 2008; Mamane 2016; Salze et al. 2018; Sani 2020). This trapping of uranium can also take place at redox fronts created through normal faults, lineaments or natural barriers (claystone zones) (Gerbeaud 2006; Billion 2014; Mamane 2016) and then, form a primary uranium mineralization deposit or secondary enrichment (Sani 2020; Mamane et al. 2019 and 2022). In the Ingall sector all holes drilled east of the N-S flexure-fault are negative (no mineralization). This confirms the screen role for uranium mineralization played by this N-S structure. For such lenticular mineralization deposits, the general orientation of the lenses (deposits) is parallel to the channels direction (Cazoulat 1985), such as uranium deposits on the Colorado Plateau in the USA and

Westmoreland in Australia (Cuney et al. 2021). This lenticular shape of uraniferous deposits of the Ingall sector shows a paloegeographic control of this mineralization. In addition, the results of this study have shown that the distribution of mineralization is strongly influenced by the horst and graben structures of the Ingall sector. A similar deposit model was highlighted in the DASA sector, in the east of the Tim Mersoï basin (Sani 2020). Indeed, the graben structure of the DASA sector, in relation with tectonic and geochemical factors and the fluids circulation, favoured the set up of mineralization deposit with high uranium contents (Sani et al. 2022).

5. Conclusion

This study combined airborne and ground radiometric surveys, drilling and logging techniques, to demonstrate the existence of uranium mineralization in the Ingall area. This study shows that these mineralizations are in the form of lenses disseminated in the fine-grained clayey and analcimonious sandstone of Assaouas formation and the medium-grained to coarse-grained sandstone with clay and/or analcimonious cement of Tchirezrine-2 formation. These lenticular ore bodies mineralization would have been set up in favour of palaeoreliefs (irregular depressions), chemical control (reducing elements) and tectonic structures (normal faults). The latter would have an additional impact on the distribution of this mineralization: In subsurface in the central part and deeper in the west of the study area.

REFERENCES

[1] Billion S (2014). Clay minerals in the uranium deposit of Imouraren (Tim Mersoï Basin, Niger): Implications on the genesis of the deposit and on the optimization of the ore treatment processes. Thesis Solid earth and surface envelopes, University of Poitiers.

[2] Cazoulat M (1985) Geologic environment of the uranium deposits in the Carboniferous and Jurassic sandstones of the Western margin of the Aïr mountains in the Republic of Niger. In: Geological environments of sandstone-type uranium deposits. IAEA-TECDOC 328, Vienna, Pp.247-263.

[3] Cuney M, Mercadier J and Bonnetti C (2021) Classification of sandstone-related uranium deposits. Journal Of Earth Science. www.earth-science.net.

[4] Forbes P (1989) Role of sedimentary and tectonic structures, regional alkaline volcanism and diagenetic-hydrothermal fluids for the formation of U-Zr-Zn-V-Mo mineralization at Akouta (Niger). Doctoral thesis, University of Burgundy, 375p.

[5] Gerbeaud O (2006) Structural evolution of the Tim Mersoï Basin: Deformations of the sedimentary cover, Relations with the location of uranium deposits in the Arlit sector (Niger). Doctoral thesis University of Paris-Sud scientific UFR of Orsay, 270p.

[6] Greigert J, Pougnet R (1967) Essay describing the geological formations of the Republic of Niger: Paris, Editions du BRGM, 273p.

[7] Joulia F (1963) Geological reconnaissance map of the western sedimentary border of the Aïr at 1/500,000. BRGM Publishing, Orléans (France).

[8] Konaté M, Denis M, Yahaya M, Guiraud M (2007) Extensive Devonian-Dinantian structuring of the Tim Mersoı basin (western border of the Aır, northern Niger): University of Ouagadougou. Annals, Series C, 5, 32.

[9] Konaté M, Ahmed Y, Harouna M (2019) Structural evolution of the Téfidet trough (East Aïr, Niger) in relation with the West African Cretaceous and Paleogene rifting and compression episodes. Geoscience Proceedings, 351(5), 355-365.

[10] Mamane MM (2016) The metallogenic system of uranium deposits associated with the Arlit fault (Tim Mersoï Basin, Niger): diagenesis, fluid circulations and metal enrichment mechanisms (U, Cu, V). Doctoral thesis, University of Lorraine, 402p.

[11] Mamane MM, Cathelineau M, Deloule E, Schimtt R, Brouand M (2019) Cenozoic oxidation episodes in West Africa at the origin of the in situ supergene mineral redistribution of the primary uranium ore bodies (Imouraren deposit, Tim Mersoï basin, Northern Niger) , Mineralium deposita. https://doi.org/10.1007/s00126-019-00945-w.

[12] Mamane MM, Cathelineau M., Deloule E., Reisberg L., Cardon O., Vallance J. and Brouand M. (2022). The Tim Mersoï basin uranium deposits (Northen Niger): Geochronology and genetic model. Ore Geology Reviews, V145.https://doi.org/10.1016/j.oregeorv.2022.104905.

[13] Moussa Y (1992) Sedimentary dynamics of Guezouman and underlying Visean formations in connection with tectonics, volcanism and climate, paleoenvironment of uranium deposits at Arlit (Niger). Doctoral thesis, University of Burgundy, 159p.

[14] Salze D (2008) Study of the interactions between uranium and organic compounds in hydrothermal systems. Thesis from the University of Nancy, 316p.

[15] Salze D, Belcourt O, Harouna M (2018) The first stage in the formation of the uranium deposit of Arlit, Niger: Role of a new non-continental organic matter. Ore Geology Reviews 102 (2018) 604–617.

[16] Sanda CMM, Moussa DDB, Mallam MH, Sani A, Lawali IC, Sofiyane AA, Gambo RN (2022) Characterization of the host sequences of uranium mineralization in the Moradi sector, Tim Mersoï basin (Northern Niger). Journal of Research in Environmental and Earth Sciences Volume 8 ~ Issue 6 (2022) pp: 70-82.

[17] Sani A, Konaté M, Dia Hantchi K, Wollenberg (2020) Polyphasic tectonic history of the N70° DASA Graben (northern, Niger). Global Journal of Earth and Environmental Science 5(3):58-72.

[18] Sani A (2020) Role of N70° accidents in the emplacement of uranium mineralization in the Tim Mersoï basin: case of the DASA graben, western border of the Aïr (Northern Niger). Doctoral thesis, Abdou Moumouni University of Niamey (Niger), 233p.

[19] Sani A, Konaté M, Dia Hantchi K and Wolenberg P (2022) Tectono-Sedimentary Evolution of Uranium Deposits in the DASA Graben (Northern Niger). Advances in Geophysics, tectonics and Petroleum Geosciences, Advances in Science, Technology & Innovation, pp: 649-654. https://doi.org/10.1007/978-3-030-73026-0_144.

[20] Valsardieu C (1971) Geological and paleogeographic study of the Tim Mersoï basin, Agadès region (Republic of Niger). Doctoral thesis, University of Nice, 519p.

Wagani I (2007) Uranium potential of possible volcanic sources for the formation of mineralization in the Arlit region (Niger). Thesis of the University of Paris Sud, 291p.